FRET evidence that an isoform of caspase-7 binds but does not cleave its substrate

Isaac T.S. Li [a,b], Elizabeth Pham [a], Jason (Jui-Hsuan) Chiang [a,b], Kevin Truong [a,b,*]

[a] Institute of Biomaterials and Biomedical Engineering, University of Toronto, Rosebrugh Building, 164 College Street, Room 407, Toronto, Ont., Canada M5S 3G9
[b] Edward S. Rogers Sr. Department of Electrical and Computer Engineering, University of Toronto, 10 King's College Circle, Toronto, Ont., Canada M5S 3G4

ARTICLE INFO

ABSTRACT

A caspase-7 biosensor (vDEVDc) based on FRET (fluorescence resonance energy transfer) was used to study the proteolytic properties of caspase-7, an executioner protease in cellular apoptosis. An active isoform of caspase-7 with the 56 N-terminal residues truncated (57casp7) cleaved vDEVDc at the recognition sequence, resulting in a FRET efficiency decrease of 61%. In contrast, an isoform with the 23 N-terminal residues truncated (24casp7) bound to vDEVDc but did not cleave the substrate, resulting in a FRET increase of 15%. Kinetic results showed an exponential substrate cleavage and binding curve for the 57casp7 and 24casp7 isoforms, respectively. FRET changes of the vDEVDc biosensor were also monitored in cos-7 cells upon STS-induced apoptosis. Finally, we modeled caspase-7 binding to vDEVDc and estimated a FRET emission ratio increase of 31.7%, which agrees with the 15% experimental result. We showed that two differently truncated isoforms of caspase-7 exhibit different enzymatic properties, namely binding by 24casp7 and hydrolysis by 57casp7.

© 2008 Elsevier Inc. All rights reserved.

Caspases are a family of cysteine proteases associated with cellular apoptosis with high substrate specificity [1]. In living cells, caspase-7 is expressed as a dimeric zymogen with a 23-residue N-terminal prodomain and remains as a dimer after activation [2]. During the activation process, initiator caspases, such as caspase-8, proteolyse between the large p20 and small p11 sub-units of pro-caspase-7 at the C-terminal side of Asp198 [1]. The prodomain of caspase-7 is also cleaved after the Asp23 residue. Nonetheless, the crucial cleavage in caspase-7 activation is at Asp198 since the cleavage at Asp23 alone does not produce an active caspase-7 [3]. The caspase-7 isoform truncated after Asp23 (24casp7, Fig. 1A) is thus inactive. In contrast, other studies of pro-caspase-7 showed that when truncated after Pro56 (57casp7, Fig. 1A), the resulting mutant is capable of autoprocessing itself into the active form [1,4].

In this study, we created a biosensor to measure the kinetics of caspase-7. Protein based fluorescence resonance energy transfer (FRET) caspase biosensors have been created to measure the caspase kinetics both *in vitro* and in living cells [5]. FRET is the transfer of energy that occurs through resonance between two fluorophores (one donor and one acceptor) with a spectral overlap in the donor emission and acceptor excitation [6]. The FRET efficiency ($E\%$) depends on the relative distance and orientation between the fluorophore pair [6]. FRET caspase biosensors are typically created by sandwiching a caspase recognition substrate with a cyan fluorescent protein (CFP) donor and a yellow fluorescent protein (YFP) acceptor [7,8]. Before proteolysing the substrate, the donor and acceptor are in close proximity restricted only by the short bridging substrate, which gives rise to a high FRET efficiency when excited by donor excitation. Once caspase cleaves the substrate, however, the fluorescent proteins are separated and FRET efficiency drops. By measuring the change in the FRET emission ratio (defined as the emission intensity of the acceptor divided by the donor), we can estimate the percentage of cleaved biosensors over time, which provides information on the caspase kinetics. In this paper, we show that the 57casp7 isoform cleaves our designed FRET caspase-7 biosensor, while the 24casp7 isoform binds but does not cleave.

Materials and methods

Construction of the plasmids expressing the vDEVDc (named phvDEVDctx) and v4Gc biosensors (named phv4Gctx). Using the cassette-based strategy described [9], the phvDEVDctx and phv4Gctx plasmids were created by combining five different plasmids: pCfptx [9], pVentx [9], pHistx [9], pDEVDtx, and p4Gtx. To construct pDEVDtx and p4Gtx, oligonucleotides were flanked by NcoI–SpeI on the 5′ end and NheI–XhoI on the 3′ end that

* Corresponding author. Address: Institute of Biomaterials and Biomedical Engineering, University of Toronto, Rosebrugh Building, 164 College Street, Toronto, Ont., Canada M5S 3G9. Fax: +1 416 978 4317.
E-mail addresses: isaac.li@utoronto.ca (I.T.S. Li), elizabeth.d.pham@gmail.com (E. Pham), jason.chiang@utoronto.ca (Jason (Jui-Hsuan) Chiang), kevin.truong@utoronto.ca (K. Truong).
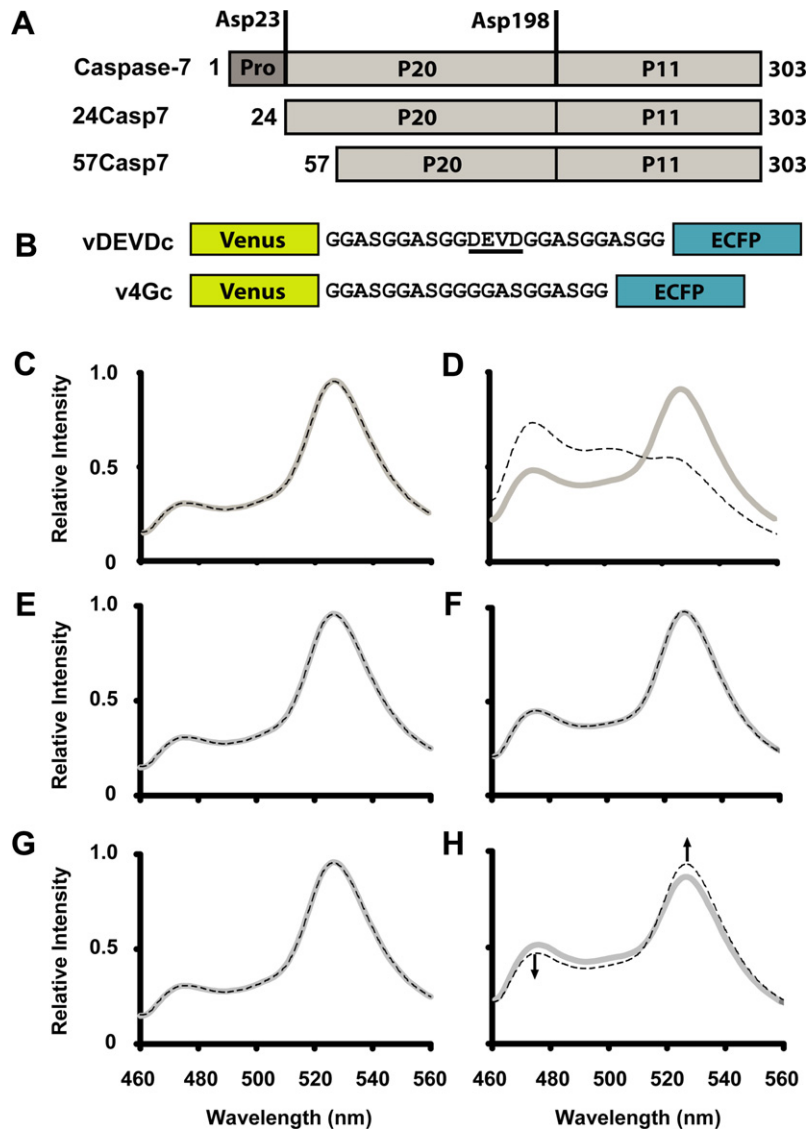
Fig. 1. Schematic diagrams and characterization of the 57casp7 isoform. (A) Schematic diagram of the caspase-7 isoforms. (B) Schematic diagram of the biosensors. The DEVD recognition sequence is underlined. The emission spectra was measured before (solid grey) and after (dotted black) an hour incubation at room temperature for (C) the 57casp7 isoform + v4Gc biosensor, (D) the 57casp7 isoform + vDEVDc biosensor, (E) the v4Gc biosensor alone, (F) the 24casp7 isoform + v4Gc biosensor alone, (G) the vDEVDc biosensor, and (H) 24casp7 + the vDEVDc biosensor. All protein concentrations were 10 ± 1 μM.

contained the peptide sequences GGASGGASGGDEVDGGASG GASGG and GGASGGASGGGGASGGASGG in human codon preference, respectively. The oligonucleotides were digested with NcoI–XhoI and ligated into the NcoI–XhoI site of pTriEx-1.1 (Novagen) to create pDEVDtx and p4Gtx. To create the intermediates pDEVDctx and p4Gctx, pCfptx was digested with SpeI–XhoI and ligated into the NheI–XhoI site of pDEVDtx and p4Gtx, respectively. To create the intermediate products pvDEVDctx and pv4Gctx, pVentx were digested with NcoI–NheI and ligated into the NcoI–SpeI site of pDEVDctx and p4Gctx, respectively. Finally, to create the phvDEVDctx and phv4Gctx, pHistx was digested with NheI–XhoI and ligated with the inserts from pvDEVDctx and pv4Gctx digested by SpeI–XhoI, respectively.

Construction of the plasmids expressing the 24casp7 (named p24casp7tx) and 57casp7 (named p57casp7tx) isoforms. The sequences of the two caspase-7 isoforms were first amplified from human skeletal muscle cDNA library by PCR using the following primers: 24casp7 forward, 5′-CGGGATCCGCTAAGCCAGACCGGTCC TCG-3′; 57casp7 forward, 5′-CGGGATCCACACATATCAGTACAACATGA ATTTTGAA-3′; 24casp7 or 57casp7 reverse, 5′-CTAGCTAGCTTGACT

GAAGTAGAGTTCCTTGGT-3′. To create the p24casp7vtx and p57casp7vtx plasmid, the PCR product for 24casp7 and 57casp7 was then subcloned into the pCfvtx plasmid cassette [9] at the BamHI and NheI sites (underlined previously), respectively. Finally, to create the p24casp7tx and p57casp7tx plasmid, Venus was excised by a PmeI digestion and self-ligation.

Protein expression. The plasmids expressing the vDEVDc biosensor, the v4Gc biosensor, 24casp7 and 57casp7 isoforms were transformed in DH5α competent cells and grown in LB + 100 μM/mL ampicillin at 37 °C for 24 h. The proteins were produced by leak expression and extracted from the cells by sonication in the buffer (50 mM Tris buffer, pH 7.5 and 100 mM NaCl). The protein concentration of each construct was estimated by fluorescence intensity and for all experiments, all protein concentrations of the isoform and biosensors were diluted to 10 ± 1 μM.

Transfection and imaging of vDEVDc in cos-7 cells. Cos-7 cells were transfected with 2 μg of phvDEVDctx using GeneJuice (Invitrogen) and incubated overnight (37 °C, 5% CO_2) in DMEM + 10% FBS on 35 mm glass-bottom wells. Cells were then washed and imaged in PBS (phosphate buffered saline) mixed with 5 mM STS. An

inverted microscope was used to collect intensity readings over a time course. The QEDInVivo software package was used to plot spectral representations of the CFP and YFP channels, as well as perform time-lapse recordings of cellular images.

Fluorescence spectroscopy. Using the fluorescence spectrophotometer (Shimadzu model RF-5301PC), the protein solution was excited at 440 nm and the emission spectrum recorded between 460 nm and 560 nm.

FRET efficiency equations. The binding event of caspase-7 to the vDEVDc biosensor is measured by the change in FRET efficiency (E%) defined as the percentage of energy transferred from the donor to acceptor from donor excitation. E% is a function of the fluorophore pairs' distance (R), Förster distance factor (R_0), and the orientation factor (κ^2):

$$E\% = \frac{R_0^6}{R_0^6 + R^6} \tag{1}$$

$$R_0 = 9.78 \times 10^3 \times (Q_d \kappa^2 n^{-4} J)^{\frac{1}{6}} \text{Å} \tag{2}$$

$$\kappa^2 = [\sin(\theta_D)\sin(\theta_A)\cos(\phi) - 2\cos(\theta_D)\cos(\theta_A)]^2 \tag{3}$$

With the parameters: quantum yield (Q_d), refractive index (n), overlap integral (J), the angle between the acceptor/donor fluorophore dipoles and the joining vector (θ_A/θ_D), and the angle between the fluorophore pair planes (ϕ).

Simulation model generation. Protein data bank (PDB) files were downloaded describing the atomic structure of yellow fluorescent protein (YFP, PDB CODE: 1MYW) [10], cyan fluorescent protein (CFP, PDB CODE: 1OXD) [11], and caspase-7 inhibitor complex (PDB CODE: 1F1J) [12]. Using FPMOD [13], we generated the model representing the vDEVDc biosensor in the absence of caspase-7 by flanking the DEVD sequence by CFP and YFP at the *N-* and *C*-termini, respectively. On the other hand, we generated the model representing the vDEVDc biosensor in the presence of caspase-7 by using the dimeric structure of caspase-7 bound to its inhibitor (PDB CODE: 1F1J). To statistically predict the FRET changes of the vDEVDc biosensor, first we generated 100 models before and after caspase-7 binding by randomly rotating the DEVD linker between CFP and YFP. Then, we calculated the E%, R, and κ^2 of each model using an ActivePerl script based on the FRET efficiency equations (above). Note that when randomly rotating the DEVD linker, the rotational freedom was restricted so that no two sub-units collided.

Results and discussion

Biosensor characterization

Our caspase-7 biosensor (vDEVDc) was cleaved by the 57casp7 isoform (Fig. 1D), while a control biosensor (v4Gc) was not (Fig. 1C). The vDEVDc biosensor consisted of a 24 amino acid linker containing the DEVD recognition sequence sandwiched between Venus [14] and ECFP (Fig. 1B). In contrast, the v4Gc control biosensor did not contain the recognition sequence (Fig. 1B). Prior to treatment with the active 57casp7 isoform, the emission spectra of both the vDEVDc and v4Gc biosensor had a strong peak emission of Venus (528 nm) due to FRET from ECFP to Venus (Fig. 1C and D). As the v4Gc biosensor had a shorter linker, it displayed a larger FRET as shown by a larger Venus emission peak relative to the ECFP (475 nm) peak in the emission spectra (Fig. 1C). After treatment of the vDEVDc biosensor with the active 57casp7 isoform, the peak emission of Venus decreased and ECFP increased due to an expected loss of energy transfer after cleavage of the biosensor (Fig. 1D). In contrast, the v4Gc biosensor was not cleaved by the 57casp7 biosensor (Fig. 1C). Therefore, these results show that

the vDEVDc biosensor was cleaved specifically by the 57casp7 isoform.

FRET changes of the vDEVDc biosensor in cells

The vDEVDc biosensor was transfected into cos-7 cells and fluorescent signals were monitored on a fluorescence microscope. Apoptosis was induced by introducing 5 mM of STS (staurosporine) to the solution. Cell morphology changes initiated by apoptosis were monitored for 6.5 h (Fig. 2A and B) while cells were excited at the CFP excitation wavelength of 438 nm. Two fluorescent channels were monitored throughout the imaging experiment to measure the signal intensity of CFP emission (483 nm) and YFP emission (520 nm). At 2 h, significant morphology changes occurred, indicating the activation of apoptotic changes within the cell. At this point, dramatic changes in the CFP/YFP fluorescent signals are observed (Fig. 2C). The YFP signal undergoes a rapid intensity decrease with a corresponding CFP signal increase. This observation demonstrates the drop in FRET efficiency upon cleavage of the vDEVDc biosensor and separation of its fluorescent pair.

Characterization and kinetics of the caspase-7 isoforms

The 24casp7 isoform had no protease activity *in vitro*, but recognized and bound to the substrate of the vDEVDc biosensor (Fig. 1E–H). A spectrum was recorded immediately after mixing the 24casp7 isoform with both the vDEVDc and v4Gc biosensors. After
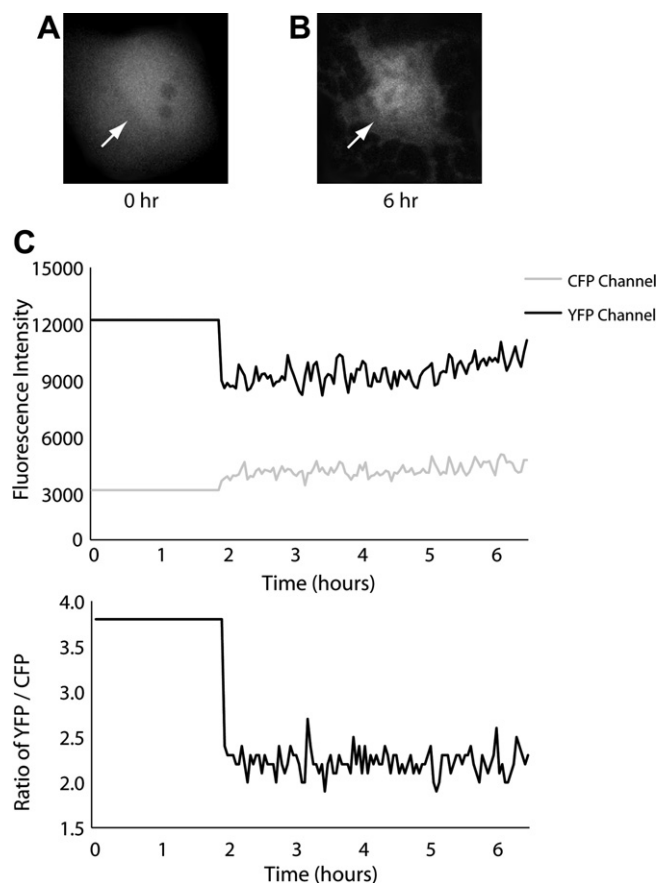
Fig. 2. Transfection of the vDEVDc biosensor. Cos-7 cells were transfected with the vDEVDc biosensor before (A) and after (B) STS-induced apoptosis with arrows indicating where fluorescence intensities were measured during the course of the experiment. CFP and YFP fluorescence channels were monitored during apoptosis for 6 h (C), with cleavage of the vDEVDc biosensor occuring at 2 h. YFP/CFP ratio changes are also shown.

incubating for an hour at room temperature, the spectrum of this solution was recorded again. Comparing the two spectra before and after the incubation period, we observed that the FRET emission ratio of the vDEVDc biosensor increased by 15% (Fig. 1H). This increase of FRET indicated a conformational change in the biosensor that did not involve proteolytic cleavage. In order to isolate the cause of the increase in FRET observed for the 24casp7 isoform, two control experiments were performed. In the first experiment, both the v4Gc and vDEVDc biosensor were incubated alone for 1 h at room temperature. The emission spectra did not change during this period (Fig. 1E and G). This shows that any changes to the spectrum over time were not caused by intrinsic properties of the v4Gc and vDEVDc biosensors. In the second experiment, the 24casp7 isoform was mixed with the v4Gc control biosensor and incubated for an hour. The spectra from before and after this incubation period were also identical (Fig. 1F). This result verifies that the 24casp7 isoform does not interact with the v4Gc biosensor, which lacks the DEVD recognition sequence. Therefore, the vDEVDc biosensor specifically interacted with the 24casp7 isoform through the DEVD recognition sequence of the vDEVDc biosensor. Since this interaction was not due to cleavage of the DEVD recognition sequence, the change in FRET emission ratio is thus due to the 24casp7 isoform binding the DEVD sequence.

In time-lapsed experiments, the 24casp7 and 57casp7 isoforms were found to exponentially bind and cleave the vDEVDc biosensor, respectively (Fig. 3). Similar controls to the above experiments
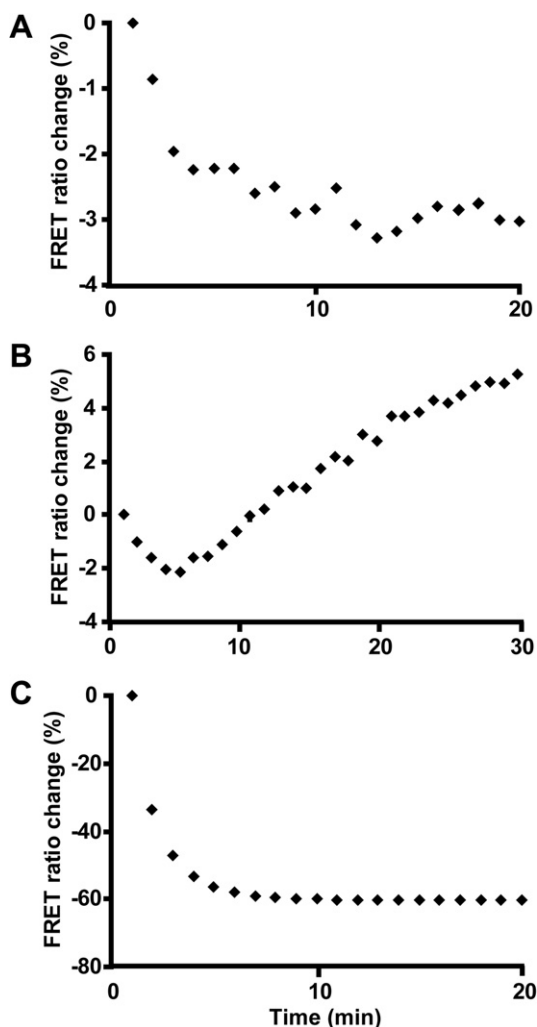
were used to obtain the time-lapsed spectra using an excitation wavelength of 440 nm every minute over a period of 20–30 min. In these time-lapsed experiments, the solution was repeatedly sampled leading to inevitable photobleaching effects. For example, in the control experiment of the vDEVDc biosensor alone, there was a FRET emission ratio decrease of 2.5% from the photobleaching effect (Fig. 3A). A similar photobleaching effect was observed in experiments with the v4Gc biosensor (data not shown). As this effect was omnipresent in time-lapsed spectra, the measured FRET emission ratio was the result of both photobleaching and bioactivity of the isoform. Further experiments of the 57casp7 isoform with our vDEVDc biosensor, as expected, showed a 67% exponential decrease of the FRET emission ratio (Fig. 3C). In contrast, experiments of the 24casp7 isoform with the vDEVDc biosensor showed an 8% exponential increase of FRET (Fig. 3B). The FRET emission ratio decrease from photobleaching was evident during the first 4 min but was overshadowed by the exponential FRET emission ratio changes in both experiments. These results indicate that the binding between the 24casp7 isoform and the vDEVDc biosensors occurred exponentially.

Computational modeling of the 24casp7 isoform binding to the vDEVDc biosensor

Computational models of the vDEVDc biosensor before and after binding to caspase-7 estimated a FRET emission ratio of ∼31.7% which is consistent with our experimental result of 15% (Fig. 4). The binding of caspase-7 to its inhibitor was used to model the binding of the vDEVDc biosensor to the active site of the 24casp7 isoform [12]. Both the caspase-7 free and bound cases had relatively low median FRET efficiency (E%) values at approximately 3%, however, at least 15% of the models in the caspase-7 bound case had a greater propensity for models with an E% larger than 20% which explained the corresponding shifts in their mean E%. For the caspase-7 free case, the average E% was 7.8% with corresponding distance and orientation factors values of 74.8 ± 10 Å and 0.470, respectively. Note that the distance factor displayed a Gaussian-like distribution whereas the orientation factor distribution was more scattered. One commonly used constant for κ^2 is 0.475, assuming the donor–acceptor orientations do not change during the lifetime of the excited state [15]. Our simulation results for orientation factor were consistent with that assumption since the orientation of the donor–acceptor pair has a large rotational freedom around the flexible linker in the caspase-7 free case. For the caspase-7 bound case, however, based on the dimer conformation of caspase-7, the E% could originate from the intra- or intermolecular FRET effect. The simulated E%, distance factor, and orientation factor averages for the intra- and inter-molecular FRET effects were 15.3%, 71.7 ± 17 Å, 0.594 and 3.4%, 98.9 ± 17 Å, 0.559, respectively. Since the intra-molecular FRET was almost fivefold compared to the inter-molecular effect due to the smaller distance factor, the intra-molecular effect was the dominant factor in the resultant E% distribution. Note also that both κ^2 values deviated from the constant 0.475 in the caspase-7 free case. This was expected because the donor–acceptor pair has reduced rotational freedom due to dimer conformation of the caspase-7 and the vDEVDc biosensor complex. The change in FRET emission ratio was estimated using the same procedure used in [13]. Since the increase in FRET efficiency is 7.5%, there is an approximately 31.7% increase in FRET emission ratio after caspase-7 binding.

Conclusion

We designed the vDEVDc biosensor for monitoring caspase-7 activity and discovered that it responds differently to two isoforms

Fig. 3. Time-lapsed experiments of (A) the vDEVDc biosensor, (B) the 24casp7 isoform + vDEVDc biosensor, and (C) the 57casp7 isoform + vDEVDc biosensor.
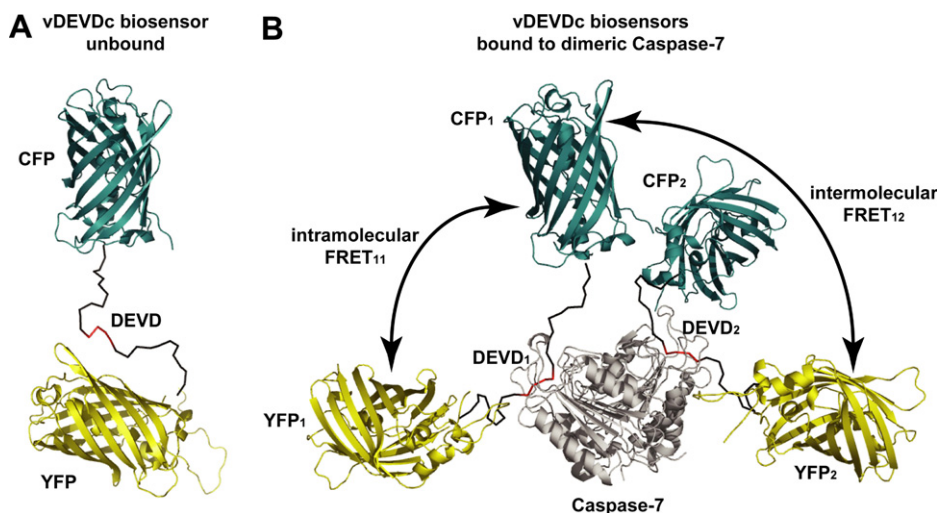
Fig. 4. Computational modeling of the vDEVDc biosensor. (A) Unbound vDEVDc biosensor, consisting of the DEVD peptide sandwiched by CFP and YFP. (B) vDEVDc biosensors bound to dimeric caspase-7 undergo both intra-molecular and inter-molecular FRET.

of caspase-7—24casp7 and 57casp7. The 57casp7 isoform exhibited the normal proteolytic activity and caused the vDEVDc biosensor to lose FRET. The 24casp7 isoform, on the other hand, caused the FRET emission ratio of vDEVDc to increase by 15%. We isolated the cause of this FRET increase to the putative binding of the 24casp7 isoform to the DEVD substrate in our vDEVDc biosensor. Furthermore, our experiments showed that upon incubating with the 24casp7 isoform, the FRET of the vDEVDc biosensor increases exponentially over time, which resembles the kinetics of a typical binding reaction. To further test the binding hypothesis, we simulated the FRET change of the vDEVDc biosensor before and after binding to caspase-7 yielding a 31.7% increase, which agreed with the 15% FRET emission ratio increase observed experimentally. Hence, we conclude that 24casp7 isoform lacks its native proteolytic activity but is capable of recognizing and binding to its substrate. Lastly, this work expands the application of caspase FRET biosensors to a different aspect of caspase activity beyond proteolysis.

Authors' contributions

ITL performed the subcloning, the spectroscopy experiments and drafted the manuscript. E.P. and J.C. performed the computational modeling and helped in the drafting of the manuscript. K.T. helped in the design of experiments and supervised the work. All authors read and approved the final manuscript.

Acknowledgments

References

[1] G.M. Cohen, Caspases: the executioners of apoptosis, Biochem. J. 326 (Pt 1) (1997) 1–16.
[2] M. Los, H. Walczak, Caspases: Their Role in Cell Death and Cell Survival, Landes Bioscience, Kluwer Academic/Plenum Pub., Georgetown, TX, New York, 2002.
[3] Y. Shi, Mechanisms of caspase activation and inhibition during apoptosis, Mol. Cell 9 (2002) 459–470.
[4] Y. Yaoita, Inhibition of nuclear transport of caspase-7 by its prodomain, Biochem. Biophys. Res. Commun. 291 (2002) 79–84.
[5] J. Zhang, R.E. Campbell, A.Y. Ting, R.Y. Tsien, Creating new fluorescent probes for cell biology, Na. Rev. Mol. Cell Biol. 3 (2002) 906–918.
[6] K. Truong, M. Ikura, The use of FRET imaging microscopy to detect protein–protein interactions and protein conformational changes in vivo, Curr. Opin. Struct. Biol. 11 (2001) 573–578.
[7] J.J. Chiang, K. Truong, Computational modeling of a new fluorescent biosensor for caspase proteolytic activity improves dynamic range, IEEE Trans. Nanobiosci. 5 (2006) 41–45.
[8] J.J. Chiang, K. Truong, Using co-cultures expressing fluorescence resonance energy transfer based protein biosensors to simultaneously image caspase-3 and Ca^{2+} signaling, Biotechnol. Lett. 27 (2005) 1219–1227.
[9] K. Truong, A. Khorchid, M. Ikura, A fluorescent cassette-based strategy for engineering multiple domain fusion proteins, BMC Biotechnol. 3 (2003) 8.
[10] A. Rekas, J.R. Alattia, T. Nagai, A. Miyawaki, M. Ikura, Crystal structure of venus, a yellow fluorescent protein with improved maturation and reduced environmental sensitivity, J. Biol. Chem. 277 (2002) 50573–50578.
[11] J. Hyun Bae, M. Rubini, G. Jung, G. Wiegand, M.H. Seifert, M.K. Azim, J.S. Kim, A. Zumbusch, T.A. Holak, L. Moroder, R. Huber, N. Budisa, Expansion of the genetic code enables design of a novel "gold" class of green fluorescent proteins, J. Mol. Biol. 328 (2003) 1071–1081.
[12] Y. Wei, T. Fox, S.P. Chambers, J. Sintchak, J.T. Coll, J.M. Golec, L. Swenson, K.P. Wilson, P.S. Charifson, The structures of caspases-1, -3, -7 and -8 reveal the basis for substrate and inhibitor selectivity, Chem. Biol. 7 (2000) 423–432.
[13] E. Pham, J. Chiang, I. Li, W. Shum, K. Truong, A computational tool for designing FRET protein biosensors by rigid-body sampling of their conformational space, Structure 15 (2007) 515–523.
[14] T. Nagai, K. Ibata, E.S. Park, M. Kubota, K. Mikoshiba, A. Miyawaki, A variant of yellow fluorescent protein with fast and efficient maturation for cell-biological applications, Nat. Biotechnol. 20 (2002) 87–90.
[15] Z. Hillel, C.W. Wu, Statistical interpretation of fluorescence energy transfer measurements in macromolecular systems, Biochemistry 15 (1976) 2105–2113.